Scripta Materialia 222 (2023) 115040

Contents lists available at ScienceDirect

Scripta Materialia

journal homepage: www.journals.elsevier.com/scripta-materialia

Discovery of core-shell quasicrystalline particles

Tong Yang [a,b], Yi Kong [a], Yong Du [a], Kai Li [a,*], Dominique Schryvers [b,*]

[a] State Key Laboratory of Powder Metallurgy, Central South University, Changsha 410083, China
[b] Electron Microscopy for Materials Science (EMAT), University of Antwerp, Antwerp B-2020, Belgium

ARTICLE INFO

Keywords:
Quasicrystal
Core-shell
Precipitation
High-angle annular dark field (HAADF)
Electron diffraction

ABSTRACT

Submicron-sized quasicrystalline particles were obtained in an Al-Zn-Mg-Cu alloy produced by traditional melting. These particles consist of an Al-Fe-Ni core and a Mg-Cu-Zn shell and were found to be stable and embedded randomly in the Al matrix. The diffraction patterns of these core-shell particles reveal a decagonal core and an icosahedral shell with, respectively, ten- and five-fold axes aligned. High resolution scanning transmission electron microscopy of the Mg-Cu-Zn shell confirms the five-fold symmetry atomic arrangement and the icosahedral structure. It can therefore be concluded that Fe and Ni impurities play an important role in mediating the formation of such an unusual ternary core-shell quasicrystalline particle. These findings provide some novel insights in the formation of quasicrystals in traditional industrial Al alloys.

Quasicrystals (QCs) are long-range ordered solids that show non-periodic symmetries, such as five-fold rotations [1]. Since the discovery in 1984 of the icosahedral phase with a fivefold symmetry in a rapidly solidified $Al_{86}Mn_{14}$ alloy by Shechtman et al. [2], the concept of QCs has attracted more and more attention. Most icosahedral single QCs with long-range orientational order and non-crystallographic point-group symmetry $m\bar{3}5$ have been discovered in rapidly solidified binary or ternary alloys [3,4]. In 1985, Bendersky [5] reported another QC which has a non-crystallographic point group (10/m or 10/mmm) together with long-range orientational order and one-dimensional translational symmetry, thus belonging to the cylindrical family of groups G_1^3. He defined this kind of QCs as decagonal QCs, which were also found in Al-Mn alloys. Nowadays, QCs are classified as three-dimensional (3D), two-dimensional (2D), and one-dimensional (1D) based on the dimensionality of their quasiperiodicity [6,7]. The icosahedral phase is the only 3D QC found, while octagonal, decagonal, and dodecagonal phases are the three types of 2D QCs discovered until now. Different examples of 1D QCs have also been found in various systems [8,9].

Icosahedral quasicrystals (IQCs) and decagonal quasicrystals (DQCs) constitute a vast majority of the QCs known so far, and have been extensively studied [6,10]. Most structural investigations are focused on single QCs in alloys, although the coexistence or composite structures of IQCs and DQCs have also been reported. For example, Beeli et al. [11] obtained a sample in Al-Pd-Mn with about 40% IQC phase and 50% DQC phase by annealing at 780 °C and quenching in water. Later on, Menguy et al. [12] confirmed that a DQC phase can intergrow epitaxially in a IQC phase to form a composite structure with alternating lamella of Al-Pd-Mn. A similar coexistence of IQC-$Ga_{42}Co_{40}Cu_{18}$ and DQC-$Ga_{43}Co_{47}Cu_{10}$ was also found by Ge et al. [13], with a tip of IQC and an epitaxial DQC phase. In these systems, the coexisting IQC and DQC have the same chemical elements, but with varying compositions.

In this work, we found a route to form novel core-shell QC particles in an Al-rich matrix by traditional melting of an Al-Zn-Mg-Cu alloy. The formation of this novel core-shell structure is found to be mediated by some common impurities (Fe and Ni) in industrial alloys. Transmission electron microscopy (TEM), high-resolution scanning transmission electron microscopy (HRSTEM), and Energy-dispersive X-ray spectroscopy (EDX) have been used to characterize the core-shell particles. These exhibit a rare shape with an Al-Fe-Ni core covered by a Mg-Cu-Zn shell revealing characteristics of both DQC and IQC structures with different compositions in both parts. Our findings provide some new perspectives and understandings of QC particles influenced by common industrial treatments and impurities.

The sample preparation and characterization methods are detailed in the Supplementary document. As a result of the hot rolling and solute heat treatment, many micron- and submicron-sized particles are formed in this Al-Zn-Mg-Cu alloy (see, e.g., Fig. S1). According to the low magnification EDX mappings in Fig. S2, all particles reveal Mg, Zn and Cu enrichments. However, as shown in Fig. S3, the diffraction patterns of some particles exhibit a face-centred cubic (FCC) structure corresponding with the C15 Laves MgCuZn phase (prototype $MgCu_2$) [14,15].

* Corresponding authors.
E-mail addresses: leking@csu.edu.cn (K. Li), nick.schryvers@uantwerpen.be (D. Schryvers).

https://doi.org/10.1016/j.scriptamat.2022.115040
Received 27 June 2022; Received in revised form 5 September 2022; Accepted 5 September 2022
Available online 11 September 2022

In comparison, Fig. 1 reveals that some particles (also enriched with Mg, Zn and Cu) are showing a five-fold QC symmetry. Aside from the five-fold pattern in Fig. 1b, two different two-fold symmetry patterns have also been obtained by tilting the particle over 26.5° around the α axis (indicated in Fig. 1b), followed by a tilt of 17.6° around the β axis (indicated in Fig. 1d). As the size of the particle is about 200–300 nm, which is close to the minimum size of the selected area electron diffraction (SAED) aperture on the Tecnai instrument, these diffraction patterns have been obtained by covering the whole area of the particle. However, the observed combination of five-fold and two-fold symmetry patterns does not correspond to any known QC symmetry. Still, the two-fold patterns and the angle between these are characteristic of a cylindrical shaped decagonal symmetry [6,7]. Indeed, according to the 2D decagonal model displayed in Fig. 1e, the angle between each edge is exactly 18°, corresponding to the tilt angle β of 17.6° in our experiment. However, if the entire particle would be shaped as the 2D decagonal prism, the five-fold symmetry pattern would be found at 90° tilting from both two-fold patterns, i.e., the viewing direction of Fig. 1e. On the other hand, the two-fold symmetry diffraction pattern in Fig. 1c is also found in many IQCs, as reported before [2,16–18]. Moreover, the previous reported spatial angle in an IQC between two adjacent five-fold directions is about 63.5° [2], which is found to be exactly the complementary angle of our tilting α angle 26.5°, as shown in Fig. 1b,d. In other words, the diffraction patterns of this particle combine the common features of IQC and DQC, which implies that this particle is hard to be defined as a single IQC or DQC structure.

According to the EDX mapping shown in Fig. 2 of the same QC particle as in Fig. 1, it is clear that the major elemental enrichments are Mg, Zn and Cu. The observed S shape (indicated with a dashed line in Fig. 2a) with clear C and O enrichments in the HAADF and full mapping images (Fig. 2a,b) is considered to be an electro-polishing artifact, caused by corrosion or etching. Meanwhile, after a longer collection time of about 20 min, some tiny Fe and Ni enrichments were observed in the middle area, defined as a core area in this particle. Moreover, in the core region where Fe and Ni are enriched, the Mg, Zn and Cu maps show some depletion, while at the same time some Al enrichment is present. The latter is clearer after a more detailed quantification by QMAP in the Esprit software, as shown in Fig. S4, together with a 2D line scan covering the core area. Although the overall concentration of Fe and Ni in this alloy is only 0.089% and 0.11%, respectively, as measured by ICP-OES, with Fe always being an inevitable impurity element in industrial Al alloys, it seems that some particles contain an Al core with Fe and Ni enrichment, and that Mg, Cu and Zn enriched regions form a shell around this core. In contrast, particles without the Al-Fe-Ni core and only enriched in Mg, Cu and Zn show the C15 Laves phase MgZnCu FCC structure (see Fig. S3). There are also many previous investigations of DQC, reported in the ternary Al-Ni-Co/Fe/Cr system [19–23], which hints to a possible DQC structure of the Al-Fe-Ni core explaining part of the diffraction patterns shown in Fig. 1. Clearly, the tiny Fe and Ni impurities play an important role in the formation of these core-shell QC particles. However, the shell structure enriched with Mg, Cu and Zn elements needs to be further confirmed as it has not been found before in the QC family system.

In order to allow high-resolution imaging of this particle, FIB was used to further thin down this electropolished area. According to the EDX mapping of this same particle after FIB cutting, and shown in Fig. S5, the Al-Fe-Ni core has been removed by the FIB and only part of the Mg-Cu-Zn shell has remained. Diffraction patterns and their respective rotation relationships of this reduced particle are shown in Fig. 3. As we can see, in this case, a five-fold (Fig. 3b), two three-fold (Fig. 3d,f), and a two-fold (Fig. 3e) symmetry pattern were found with the expected tilt angles for an overall IQC symmetry for the remaining shell (i.e., no three-fold symmetries exist in the decagonal prism model). Indeed, as seen in Fig. 3g, tilting over 31° brings an IQC five-fold

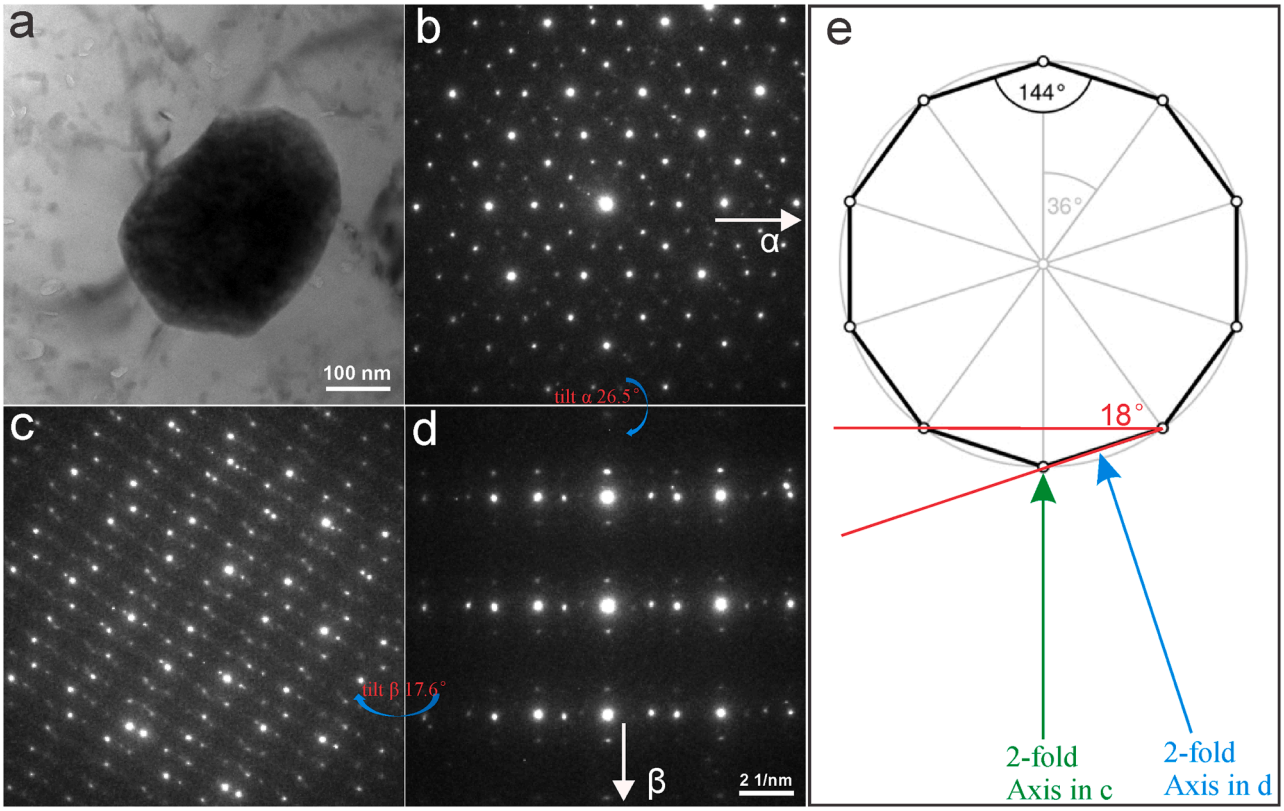

Fig. 1. Characteristic SAED patterns of a core-shell QC particle. a Bright field image of the QC particle. b-d Diffraction patterns of the particle showing five-fold and two-fold symmetry axes. e Schematic diagram of a decagon shape with indicated two-fold axes of the respective viewing directions in c and d. Scale bars in b-d are the same.

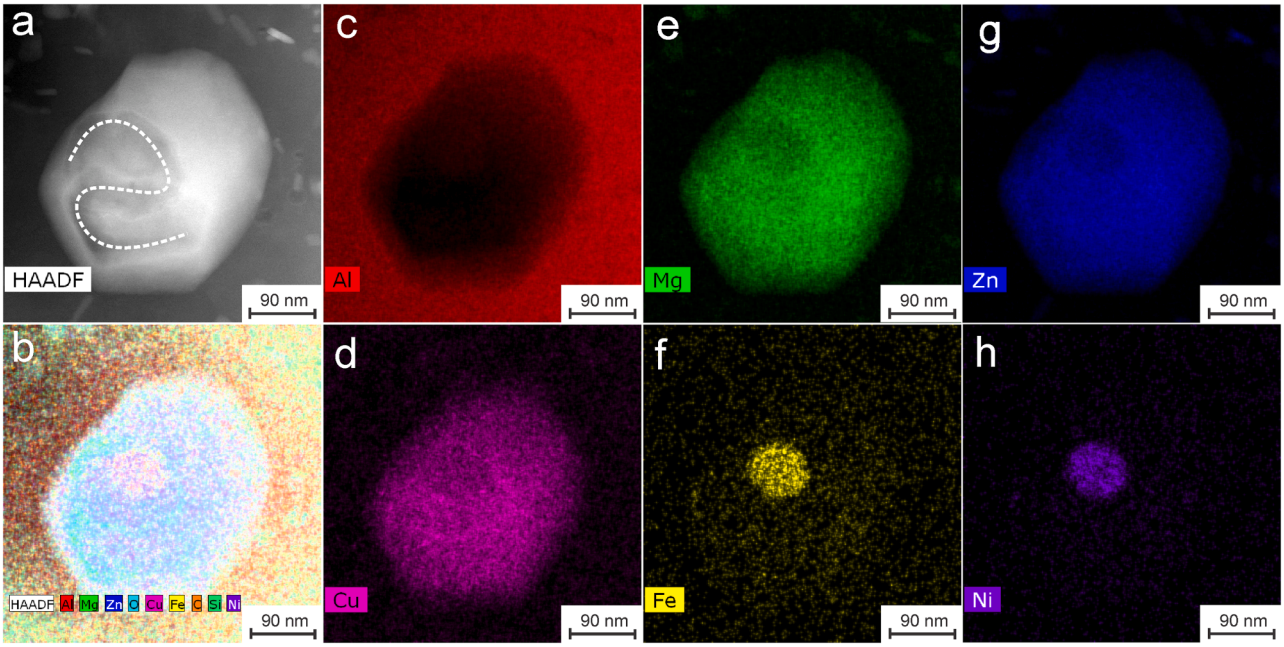

Fig. 2. EDX mappings of a core-shell QC particle. a HAADF image and b full EDX map of the QC particle of Fig. 1. Various elements are separately mapped in c to h. For maps f and h, revealing Fe and Ni enrichments, respectively, in the centre of the particle, a longer collection time (20 min) was used.

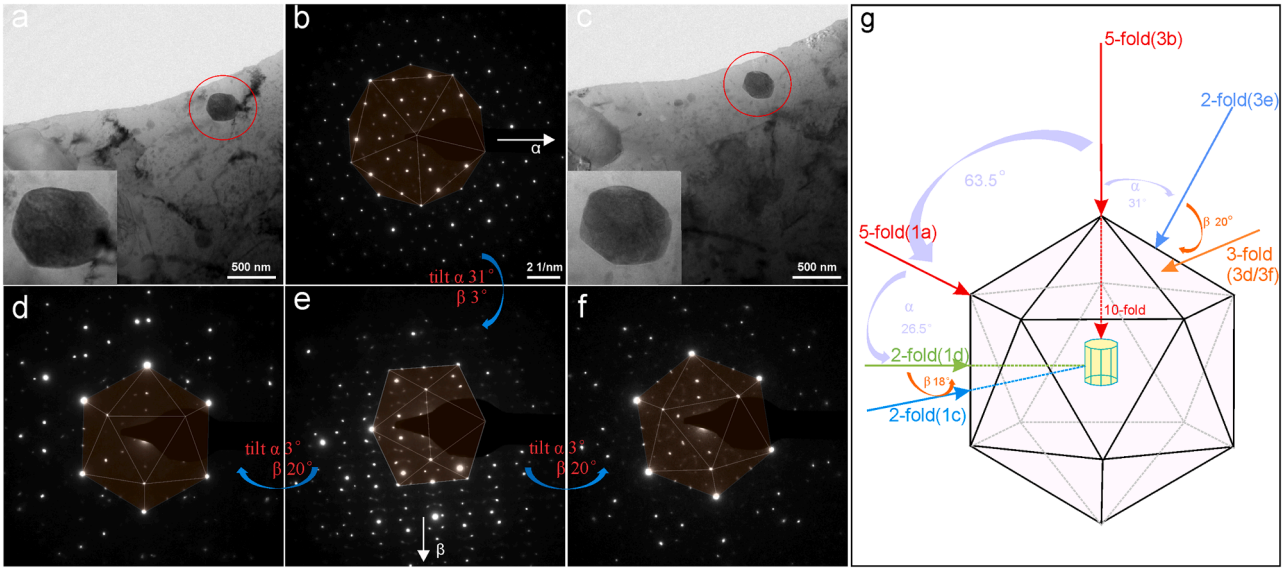

Fig. 3. Bright Field images and diffraction patterns of the particle in Fig. 1 after continued FIB cutting. a BF image under five-fold symmetry zone axis in b. b Diffraction pattern under five-fold symmetry. c BF image under two-fold symmetry axis in e. d-f Diffraction patterns under three-fold and two-fold symmetry axes. (Corresponding real-space projection shapes are overlaid on the diffraction patterns). g Schematic diagram of the IQC with a decagonal model in its core and respective angles between viewing directions. Scale bars in b and d-f are the same.

orientation into a two-fold one, with three-fold axes on both sides at 20° tilt. Combining the information from the full particle, still containing the core, and the leftover shell after FIB, the entire model for the core-shell particle shown in Fig. 3g is suggested: a decagonal core was formed with an Al-Fe-Ni content, after which an icosahedral shell has grown containing primarily Mg, Cu and Zn atoms. Indeed, five-fold symmetry patterns can be obtained when viewed from the icosahedron vertexes, while DQC two-fold symmetry patterns can be found from the edges, as indicated by green and blue dashed arrows. When viewed from the plane, as indicated by the orange arrow, the IQC three-fold symmetry pattern can also be acquired. Interestingly, a DQC has been reported before in $Al_{71}Ni_{23}Fe_5$ [24] and $Al_{75}Ni_{10}Fe_{15}$ [19] but no IQC phase has been observed in Mg-Cu-Zn so far, which can explain why the pure Mg-Cu-Zn particles do not show a QC symmetry, but grow with the C15 Laves phase structure. In other words, the Mg-Cu-Zn IQC shell formed in an epitaxial manner on the Al-Fe-Ni DQC core and remained stable under the present treatment conditions. The alignment of the five- and ten-fold axes in the IQC shell and DQC core, respectively, is in agreement with earlier findings on coexisting QC structures [12,13]. It should further be mentioned that, as shown in Figs. S6 and S7 by diffraction patterns and HRTEM images, no orientation relationship exists between the core-shell particle and the Al matrix.

In Fig. 4, high-resolution HAADF-STEM images of this same particle after FIB cutting are shown. Both the central area and edge area have

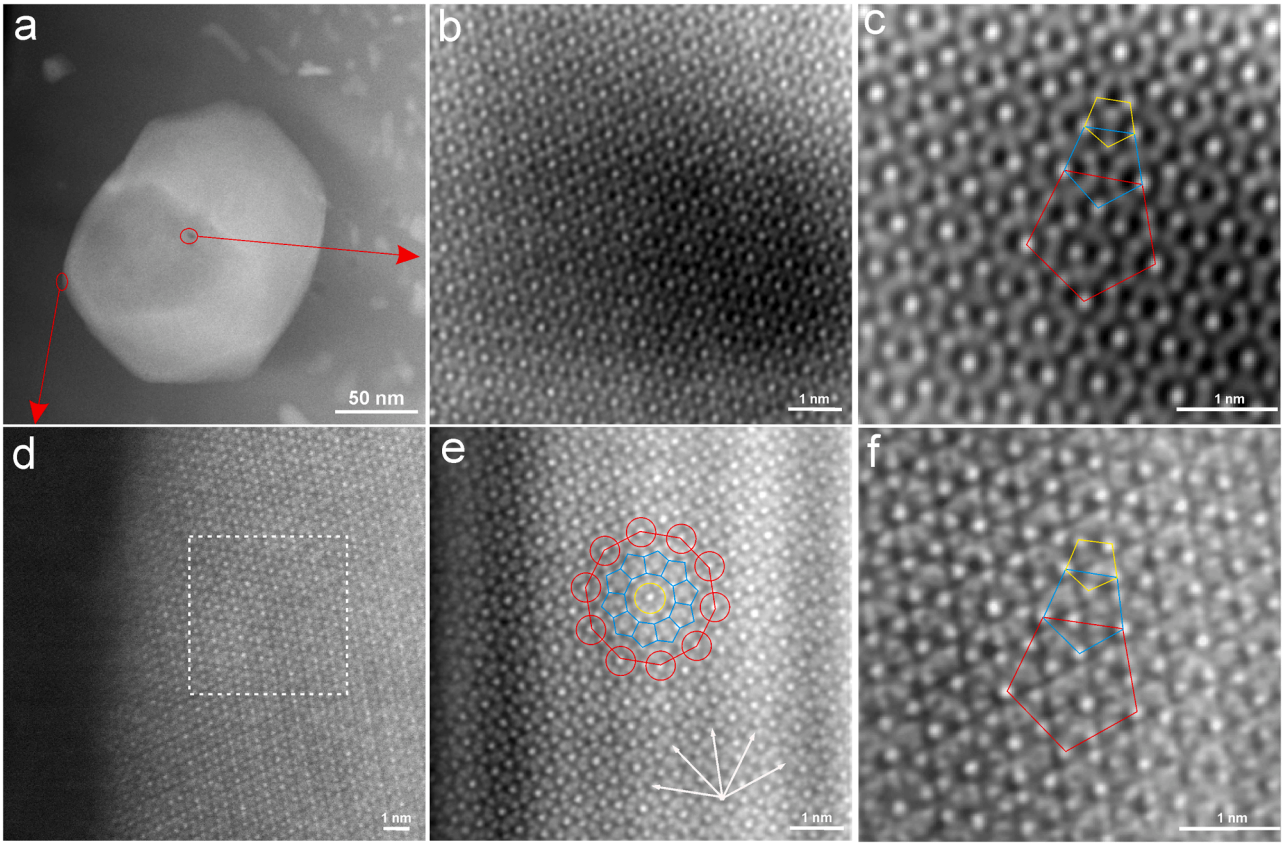

Fig. 4. Low-magnification HAADF-STEM image of the particle after FIB cutting in a and its corresponding atomic-scale images. b-c High-resolution HAADF-STEM images of the central structure, c is the enlarged area of b. d-f High-resolution STEM images of the shell structure, e and f are enlarged areas.

been investigated to verify the atomic structure. Fig. 4a shows the morphology of this QC particle under a five-fold symmetry zone axis. Fig. 4b,c are obtained from the central area, as shown in Fig. 4a, and the dark spot (possibly due to beam damage) is used as a reference to track the central part of this particle. Fig. 4c is an enlarged area of Fig. 4b, where lines with pentagonal units have been overlaid to visualize the atomic five-fold symmetry structure. TEM image filters in DM3 software have been used to sharpen the images. Fig. 4d–f show the HAADF-STEM images of the shell structure. The interface between the Al matrix, seen as the black edge on the left side, and the particle is obvious in Fig. 4d, confirming that there is no orientational relationship between matrix and QC particles. Lines have also been added in Fig. 4e to analyse the Mg-Cu-Zn shell structure, revealing a combination of decagonal and pentagonal units, corresponding to the reported IQC atomic-scale structure in the Yb-Cd system [3]. Meanwhile, five axes are highlighted by white arrows in Fig. 4e. Along each axis, the distances between these atoms are not evenly spaced but do show a typical QC periodicity, as shown by the line scans in Fig. S8. An enlarged area of Fig. 4f also displays several pentagonal units of different sizes, marked with red, blue and yellow lines. These units are tiling the entire area and confirming the QC nature of the shell. The ratio between the different length sides is 1.618, also found in other QC systems and illustrating an

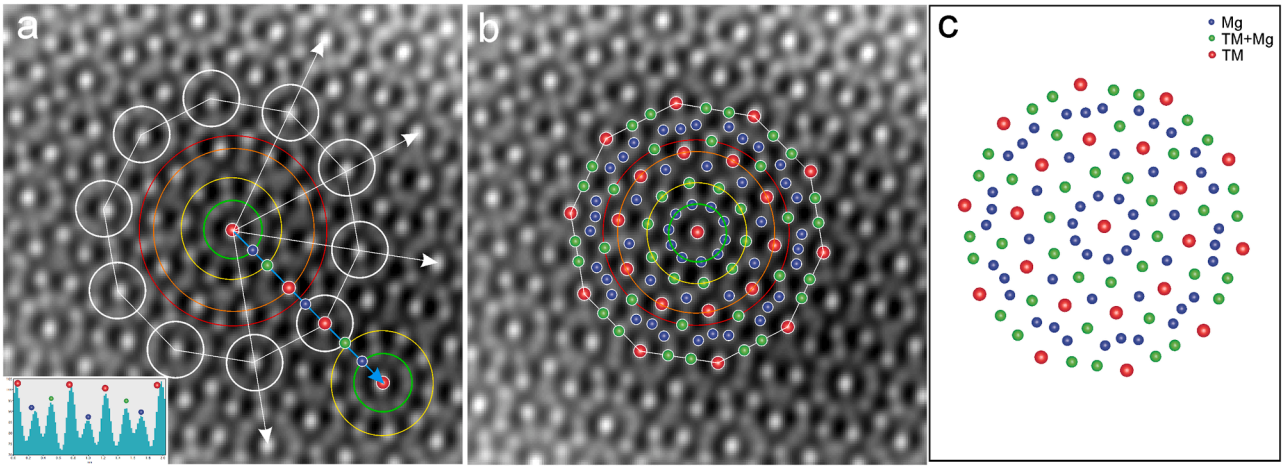

Fig. 5. Atomic structure analysis of the Mg-Cu-Zn IQC shell using HAADF-STEM images. a HAADF-STEM image with intensity line scan (along blue arrow). b Structure analysis with atoms overlaid. c Atomic model of Mg-Cu-Zn IQC.

inflation/deflation scaling rule by the golden mean τ [25–27]. Moreover, the whole crystal structure in this particle after FIB cutting is homogenous from edge to centre, forming a perfect IQC of the ternary Mg-Cu-Zn system, the core being removed by the FIB cutting.

Local structural details can be discussed based on the ultra-high-resolution STEM image under the Z-contrast condition. The potential atomic structure of the Mg-Cu-Zn QC is demonstrated in Fig. 5, supported by the intensity line scan of the atomic columns. The background intensity is weaker in the area of the black spot central part and the thickness is also more homogenous compared to the shell/edge part. The intensity maps comparison in Fig. S8 shows the same rule. Therefore, in order to get more accurate intensities of the atomic columns and a decrease of the influence of other factors, the HAADF image of the central part in Fig. 4b.c was chosen for atomic structure analysis. According to the intensity map in Fig. 5a, there are mainly 3 kinds of intensities defined as weak, medium and strong intensity, represented by different colours of atoms (blue, green and red, resp.). The atomic numbers of Cu and Zn ($Z_{Cu} = 29$, $Z_{Zn} = 30$) are too close to each other to be distinguished by the HAADF image, even when they are chemically ordered. Therefore, the positions of Cu atoms and Zn atoms might be switched and they are both commonly referred to as transition metal (TM) atoms (or columns) [21,28,29]. Therefore, the weakest intensity atom column is referred to as the Mg column ($Z_{Mg} = 12$), while the medium one is a mixed column of Mg and TM, and the strongest intensity atom column is TM. According to the periodicity principle of this Mg-Cu-Zn QC, repetitive atoms have been overlaid on the STEM images. For instance, as marked in Fig. 5a, the red TM atom is regarded as one centre of this QC structure, and then ten atoms in the first lap (from inside to outside) are denoted with a green circle, followed by yellow, orange and red circles. The space distance of a quasi-period between two centres was calculated according to the intensity maps as $0.47 + 0.29 + 0.47 + 0.76 = 1.99$ nm, in detail illustrated in Fig. S8. Therefore, another TM centre can be found at this distance, with again a TM atom (red) in the centre, as shown in the bottom-right corner of Fig. 5a. The first and second laps from this centre are again marked by a green and yellow circle, respectively, and other periodical circles can be found as well. Consequently, the atomic arrangements from one centre to another can be referred to as follows: TM-Mg-TM+Mg-TM-Mg-TM-TM+Mg-Mg-TM. More details of the structure according to the observed HAADF-STEM intensities are given in Fig. 5b,c.

In summary, a new type of QC particle with a core-shell structure and obtained by a novel route in traditional melting of Al alloys is observed and described. Our detailed conclusions are as follows:

- For the first time, submicron-sized QC particles are obtained by a traditional Al alloy process, i.e., without the use of rapid solidification or high-temperature annealing conditions.
- Impurities of Fe and Ni can mediate the formation of QC particles. Particles without Fe/Ni in the nucleation core are characterized as C15 FCC MgCuZn Laves phase. With Fe/Ni in the nucleation core, QC particles are formed.
- These QC particles can be stably embedded in the Al matrix and have a rare structure containing an Al-Fe-Ni core and a Mg-Cu-Zn shell. Diffraction patterns of these core-shell particles combine the characteristics of both DQC and IQC, with a DQC core and an IQC shell.
- High-resolution images confirm that Mg-Cu-Zn can form a perfect QC structure shell when covering or enveloping a QC core, adding a new Mg-Cu-Zn IQC system in the ternary QC family.

CRediT authorship contribution statement

Tong Yang: Conceptualization, Methodology, Investigation, Formal analysis, Writing – original draft. **Yi Kong:** Validation. **Yong Du:** Validation. **Kai Li:** Validation, Writing – review & editing. **Dominique Schryvers:** Validation, Writing – review & editing.

Declaration of Competing Interest

The authors declare no competing interests.

Acknowledgments

This work is financially supported by the National Natural Science Foundation of China (51820105001 and 52071340), and China Scholarship Council for Tong Yang's Joint-PhD program (CSC202006370239). We sincerely appreciate the support of Armand Béché, Lars Riekehr and Chuang Gao at EMAT of the University of Antwerp for the assistance in training and use of the TEM and of Saeid Pourbabak and Stijn Van den broeck for the sample preparation.

Supplementary materials

Supplementary material associated with this article can be found, in the online version, at doi:10.1016/j.scriptamat.2022.115040.

References

[1] D. Levine, Quasicrystal: a new class of ordered structures, Phys. Rev. Lett. 53 (1984) 2477–2480.
[2] D. Shechtman, I. Blech, D. Gratias, et al., Metallic phase with long-range orientational order and no translational symmetry, Phys. Rev. Lett. 53 (20) (1984) 1951–1953.
[3] H. Takakura, C.P. Gomez, A. Yamamoto, et al., Atomic structure of the binary icosahedral Yb-Cd quasicrystal, Nat. Mater. 6 (1) (2007) 58–63.
[4] M. De Boissieu, Quasicrystals: model structures, Nat. Mater. 12 (8) (2013) 692–693.
[5] L. Bendersky, Quasicrystal with one-dimensional translational symmetry and a tenfold rotation axis, Phys. Rev. Lett. 55 (14) (1985) 1461–1463.
[6] R. Li, Z. Li, Z. Dong, K. Khor, A review of transmission electron microscopy of quasicrystals—how are atoms arranged? Crystals 6 (9) (2016).
[7] E. Abe, Electron microscopy of quasicrystals - where are the atoms? Chem. Soc. Rev. 41 (20) (2012) 6787–6798.
[8] A. Jagannathan, The Fibonacci quasicrystal: case study of hidden dimensions and multifractality, Rev. Mod. Phys. 93 (4) (2021), 045001.
[9] L.X. He, Z. Zhang, K.H. Kuo, et al., One-dimensional quasicrystal in rapidly solidified alloys, Phys. Rev. Lett. 61 (1988) 1116–1118.
[10] W. Wolf, C. Bolfarini, C.S. Kiminami, et al., Recent developments on fabrication of Al-matrix composites reinforced with quasicrystals: from metastable to conventional processing, J. Mater. Res. 36 (1) (2021) 281–297.
[11] C. Beeli, H.U. Nissen, J. Robadey, Stable Al-Mn-Pd quasicrystals, Philos. Mag. Lett. 63 (2) (1991) 87–95.
[12] N. Menguy, M. Audter, M.D. Botssieu, et al., Phason-Phonon-assisted epitaxy at icosahedral-decagonal interfaces in Al-Pd-Mn quasicrystals, Philos. Mag. Lett. 67 (1) (1993) 35–41.
[13] S.P. Ge, K.H. Kuo, Icosahedral and stable decagonal quasicrystals in Ga46 23Cu23 Si8, Ga50 Co25 Cu25 and Ga46 V23 Ni23 Si8, Philos. Mag. Lett. 75 (5) (1997) 245–254.
[14] G. Yuan, H. Kato, K. Amiya, et al., Excellent creep properties of Mg-Zn-Cu-Gd-based alloy strengthened by quasicrystals and Laves phases, J. Mater. Res. 20 (5) (2005) 1278–1286.
[15] W.B. Pearson, Dimensional analysis of Laves phases: phases with the MgCu2 structure, Acta. Crystallogr. B Struct. Sci. Cryst. Eng. Mater. 37 (6) (1981) 1174, 1138.
[16] Z. Zhang, H.Q. Ye, K.H. Kuo, A new icosahedral phase with m35 symmetry, Philos. Mag. A 52 (6) (1985) L49–L52.
[17] X. Zhang, R.M. Stroud, J.L. Libbert, et al., The icosahedral and related crystal approximant phases in Ti-Zr-Ni alloys, Philos. Mag. B 70 (4) (1994) 927–950.
[18] E. Abe, A.P. Tsai, Quasicrystal-crystal transformation in Zn-Mg-rare-earth alloys, Phys. Rev. Lett. 83 (1999) 753–756.
[19] A.P. Tsai, A. Inoue, T. Masumoto, New Decagonal Al-Ni-Fe and Al-Ni-Co alloys prepared by liquid quenching, Mater. Trans. JIM 30 (2) (1989) 150–154.
[20] Y. Yang, Y. Chen, C. Dong, et al., Structure of an $Al_{64}Cu_{22}Co_{14}$ decagonal quasicrystal studied by Cs-corrected STEM, Micron 153 (2022), 103194.
[21] S. Taniguchi, E. Abe, Highly-perfect decagonal quasicrystalline $Al_{64}Cu_{22}Co_{14}$ with non-centrosymmetry, Philos. Mag. 88 (13–15) (2008) 1949–1958.
[22] S. Ritsch, Highly perfect decagonal Al-Co-Ni quasicrystals, Philos. Mag. Lett. 74 (2) (1996) 99–106.
[23] K. Hiraga, K. Yubuta, K.T. Park, High-resolution electron microscopy of Al-Ni-Fe decagonal quasicrystal, J. Mater. Res. 11 (07) (1996) 1702–1705.
[24] U. Lemmerz, B. Grushko, C. Freiburg, et al., Study of decagonal quasicrystalline phase formation in the AI-Ni-Fe alloy system, Philos. Mag. Lett. 69 (3) (1994) 141–146.
[25] H. Ma, Z. He, H. Li, et al., Novel kind of decagonal ordering in $Al_{74}Cr_{15}Fe_{11}$, Nat. Commun. 11 (1) (2020) 6209.
[26] T. Ishimasa, Y. Fukano, M. Tsuchimori, Quasicrystal structure in Al-Cu-Fe annealed alloy, Philos. Mag. Lett. 58 (3) (1988) 157–165.

[27] J. Ledieu, J.T. Hoeft, D.E. Reid, et al., Pseudomorphic growth of a single element quasiperiodic ultrathin film on a quasicrystal substrate, Phys. Rev. Lett. 92 (13) (2004), 135507.
[28] P.J. Steinhardt, H.C. Jeong, K. Saitoh, et al., Experimental verification of the quasi-unit-cell model of quasicrystal structure, Nature 396 (6706) (1998) 55–57.
[29] E. Abe, S.J. Pennycook, A.P. Tsai, Direct observation of a local thermal vibration anomaly in a quasicrystal, Nature 421 (6921) (2003) 347–350.